

Optical Measurement of the stress and flow profile of foams in an idealized deglutition

Optische Messung der Spannungs- und Strömungsprofile von Schäumen in einem idealisierten Schluckvorgang

Sascha Heitkam¹, Christoph Gerstenberg², Artem Skrypnik¹, Eric Morelle², Christopher McHardy², Cornelia Rauh²

¹ Technische Universität Dresden, Institut für Verfahrens- und Umwelttechnik, Helmholtzstr. 14, 01069 Dresden

² Technische Universität Berlin, Fachgebiet Lebensmittelbiotechnologie und -prozesstechnik, Königin-Luise Straße 22, 14195 Berlin

Flowing Foams, Elastic deformation, Image segmentation, optical measurement
Strömende Schäume, Elastische Deformation, Bildsegmentierung, optische Messtechnik

Abstract

Various physicochemical properties play a decisive role in the evaluation of foods, influencing taste, odor, texture and mouthfeel when the food is distorted. Therefore, rheological investigations of foods are used in product development to specifically improve the texture or mouthfeel of a product. Since mouthfeel describes the physical interaction between the food and various haptic sensors in the mouth during the chewing and swallowing process, it is advantageous to perform rheological measurements in geometries and under conditions that reflect the flow conditions present in the mouth. Up to now, such investigations have been limited primarily to viscous or lumpy foodstuffs. Here, foam, as a multiphase system consisting of a (highly) viscous liquid and dispersed gas, exhibits complex rheological behavior due to its compressibility. In addition, the foam undergoes partial destruction of its structure during the swallowing process, which can change its rheological properties over time.

For the imaging of the swallowing process, an experimental setup was developed consisting of a two-dimensional replica of the palate and a movable tongue based on dental impressions. Foam with different properties such as the mean bubble size and the liquid content or the degree of polydispersity can be generated. Furthermore, two tongue geometries with different roughness are available. The flow as well as the deformation of the foam is evaluated by optical methods such as PIV and particle tracking. The resulting velocity, shear rate and (wall) shear stress distributions can provide information about the haptic perception in the mouth during the swallowing process.

Introduction

Various physicochemical properties play a decisive role in the evaluation of foods, influencing taste, odor, texture, and mouthfeel. The texture of food describes a multi-parameter property including properties like viscosity, elasticity, and adhesion, which are related to food structure (Szczeniak 2002, Bourne 2002). Therefore, rheological and tribological investigations are used in product development to improve the texture or mouthfeel of food (Greis et al. 2022, Fox et al. 2021). Since mouthfeel describes the physical interaction between the food and

various haptic sensors in the mouth during the chewing and swallowing process, it is advantageous to perform rheological measurements in geometries and under conditions that reflect the flow conditions present in the mouth including the consideration of the tongue roughness (approx. 100 μm) of the tongue as well as typical speed of motion (up to 200 mm/s) (Stokes et al. 2013, Selway and Stokes 2014). Up to now, such investigations have been limited primarily to viscous or chunky foodstuffs (Rauh et al. 2012, Mathmann 2011).

Foam, as a multiphase system consisting of a (highly) viscous liquid and dispersed gas, is an important component of many foods and beverages (Murray 2020). In an oral cavity, foam can be expected to exhibit complex rheological behavior due to its compressibility and the impact of drainage on the flow behavior (Höhler and Cohen-Abbad 2005, Cohen-Addad et al. 2013). In addition, the foam undergoes partial destruction of its structure during the swallowing process, which can change its rheological properties over time. Another factor is the impact of roughness induced friction on the flow, which is particularly relevant for the textural perception (Marchard et al. 2020).

The mechanical shear and elongational forces in the human oral cavity have been modelled by simplifying the tongue-palate-region as two parallel plates, which is appropriate to describe the quench flow in the mouth during the swallowing of liquid foods (Nicosia & Robbins, 2001; Kokini, Kadane, & Cussler, 1977; Campanella & Peleg, 1987). The complexity of the kinetics of the food intake is enhanced by the motion of the tongue, as it affects the flow-induced pressure and shear stress distributions during swallowing (Rauh et al. 2012).

Although not being reported previously, it can be expected that this is also the case for the swallowing of foam. To clarify this question, we investigate the foam flow in the gap between tongue and palate by means of optical measurement techniques. In the setup, we can vary bubble size, liquid fraction, and tongue velocity. Special focus is on the influence of the tongue roughness on the flow profile of the foam. The particular shape and mode of movement is motivated by a three-dimensional numerical study of the foam flow when the tongue compresses against the palate. However, to achieve optical access, a Hele-Shaw like cell is employed. In contrast to other works on foam flow in Hele-Shaw configurations (Tong et al. 2011, Osei-Bonsu et al. 2016), the thickness of our cell is larger than the bubble diameter. Consequently, a multi-layer foam structure is formed between the plates.

Recording high-speed images of the foam movement during compression, certain flow features can be extracted and investigated. We employ adapted Particle-Image Velocimetry (PIV) and Particle-Tracking velocimetry (PTV) algorithms to measure the velocity distribution inside the flow. Also, we analyze the elastic deformation of the foam structure to measure the wall shear stress. For this, a Convolutional Neural Network (CNN) for image segmentation was developed and optical methods such as PIV and particle tracking were applied. CNN were previously shown to be suitable tools for the analysis of foams and foam structures (Panckow et al. 2021, Knüpfer and Heitkam 2022, Morelle et al. 2021). However, it is important to enable a CNN to make predictions for a wide range of foam structures and bulk liquids in order to capture the broad diversity of foam appearances.

Material & Methods

Experimental setup

The foam is confined between two acrylic glass plates of 5 mm spacing. The shape of the tongue and palate is 3D-printed from tough PLA with a resolution of 0.1 mm on an Ultimaker S5. Two different tongues are used. One has a smooth surface, and one shows 36 triangular edges of 0.66 mm height (see Figure 1).

Figure 1 sketches the geometrical setup. At the bottom, a liquid reservoir is connected to an external reservoir to maintain a constant liquid level. For liquid, tap water with 6 g/L sodium dodecyl sulfate (SDS) is used.

Bubbles are generated in the liquid reservoir by means of a needle of 0.4, 0.7 and 1.2 mm diameter, respectively, that is charged with pressurized air of 20 ml/min volumetric flow. This process yields an average bubble size of 1.79, 1.89 and 2.35 mm diameter, respectively.

In order to control the liquid fraction of the foam, identical liquid at a flow rate between 0.6 and 5.8 ml/min was injected above the tongue area into the foam by means of a needle and a peristaltic pump (Watson Marlow 114DV). This liquid drains down through the foam, yielding a stationary liquid fraction. The corresponding liquid fraction is measured simultaneously by means of a pair of electrodes below the tongue area. Following Feitosa's equation (Feitosa et al. 2005), the electrical resistance between the electrodes is transferred into liquid fraction.

In order to observe the foam movement, high speed images are captured, using a Phantom camera (Phantom VEO 410) at 1000 frames per second. The spatial resolution equals 23.2 px/mm. Diffusive backlight illumination is employed, allowing for exposure times of 500 us. A sample image is shown in figure 2.

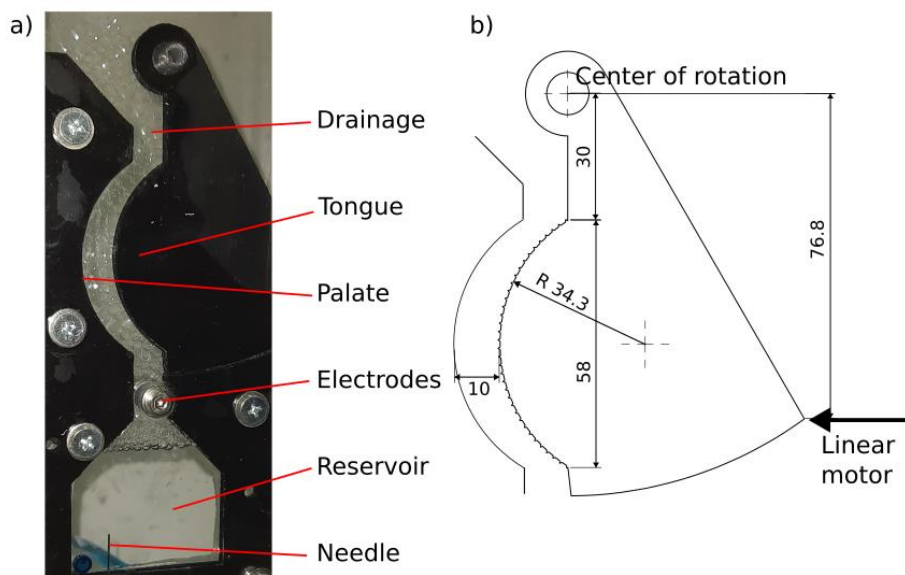


Figure 1: Picture of the setup (left) showing the point of drainage injection, the mobile tongue and fixed palate, electrodes for liquid fraction measurement, liquid reservoir and needle for bubble generation. Drawing (right) providing the precise geometry of the setup.

After starting the measurement, the tongue was pushed at constant velocity towards the palate by a linear motor (LinMot, Switzerland). Velocities between 1.25 mm/s and 10 mm/s are researched, yielding between 1000 and 8000 frames for the complete process.

Image segmentation

A convolutional neural network (CNN) based on the U-Net architecture (Ronneberger et al. 2015) was used to segment the foam images from the experiment. To adapt this CNN architecture to foam images, a custom weight loss function was implemented and optimized for the segmentation of a broad range of different foam structures. This function punishes an incorrect segmentation of the liquid phase more severely than of the gas phase and additionally emphasizes thin lamellae over thick lamellae during training. The training set consisted of 131 images of foam based on different liquids and with varying foam structures including 13 images of a

surfactant foam. To ensure that the CNN can generalize the segmentation of foam images, all images of surfactant foam were excluded from the training, thus leaving 82 images for the training and 36 for the validation. Furthermore, to achieve a robust segmentation, all training images were augmented with a random variation in brightness, contrast, sharpness, color, elastic transformation, white noise, and/or motion blur to the image. After the training, an additional validation was performed solely on the excluded surfactant foam images. Here, the relative error between the network prediction and the ground truth was 5.3 % and 5.6 % for the Sauter mean diameter and arithmetic mean diameter, respectively. This deviation may be caused by foam structures that are larger than the evaluation window of the CNN (256 x 256 px) or by objects (bubbles, lamella) that are too small to be still resolved after the image convolution. This effect was qualitatively confirmed by differently resizing images of the training set. Figure 2 shows the bubble segmentation with the CNN for both wet and dry foams with liquid fraction of 3,4 % (left) and 11.2 % (right), respectively.

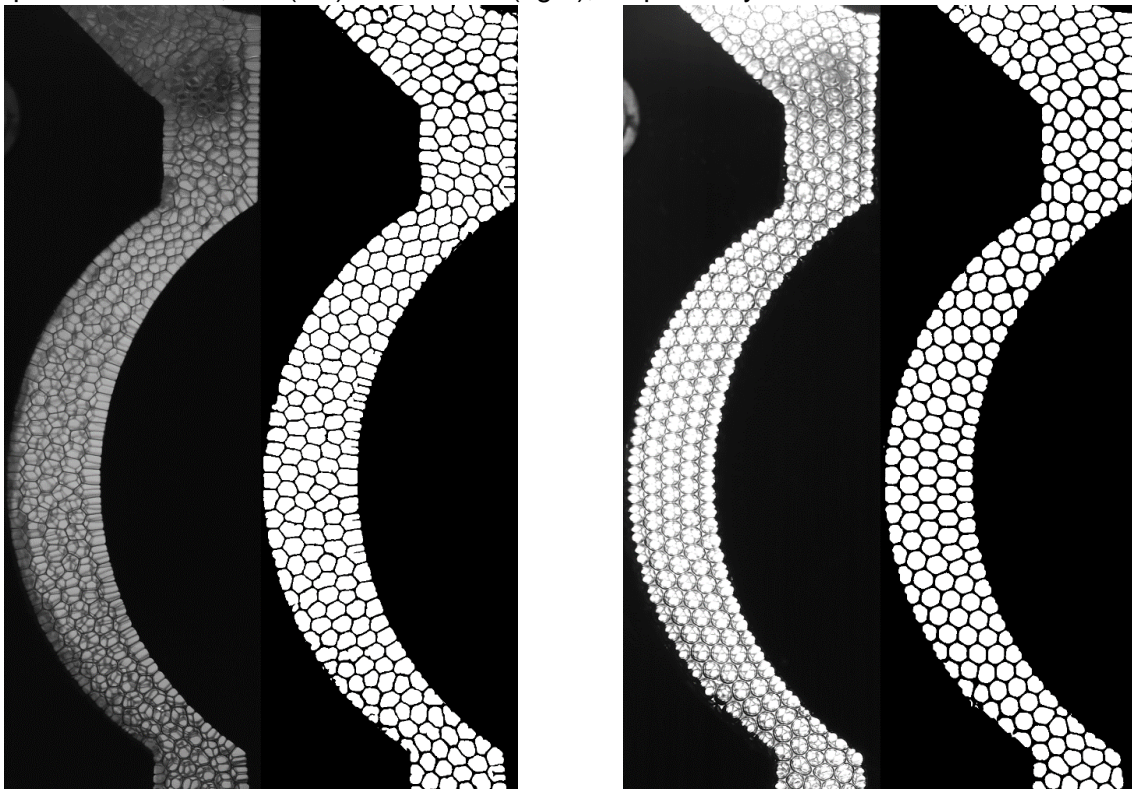


Figure 2: Examples of the bubble segmentation for foam of 1.89 mm bubble diameter at liquid fraction of 3,4 % (left) and 11.2 % (right), respectively.

Foam structure characterization

Unlike Newtonian fluids like air and water, foam constitutes a viscoelastic material (Cantat et al. 2013). At vanishing stresses, the foam structure adapts a minimum energy state corresponding to a minimum interface area. At low stresses, the foam structure deviates from this minimum state, corresponding to an elastic deformation. When the stress exceeds the critical yield stress, topological rearrangements within the foam structure occur, so-called T1 rearrangements. These T1's release some of the elastic stresses, causing the foam to yield. The elastic stresses inside the foam structure are caused by surface tension γ . Thus, one can measure the elastic stresses by analyzing the orientation of the lamellas (Dollet & Graner, 2007).

Here, we measure the wall shear stress between foam and tongue by analyzing the angle between the lamellas and the tongue surface. At zero wall shear stress, the lamellas should

orient perpendicular to the surface, following Plateaus laws (Cantat et al. 2013). However, a non-zero wall shear stress τ will tilt the lamellas by an angle φ , yielding

$$\tau = \frac{2\sin(\varphi)\gamma n_B}{S} \quad (1)$$

with n_B the number of bubbles along a certain arc length S of the wall. The factor 2 accounts for the two interfaces of each lamella.

In order to compute the wall shear stress automatically, the segmented images are used and the position of nodes on the cover plate are identified (see Figure 3). Using geometric relations, the angle φ of each wall-bounded lamella is measured and averaged over an arc length of 40 degrees in the upper third of the channel.

Bubble tracking and imaging velocimetry

To measure the velocity distribution inside the flowing foam, adapted PIV and PTV algorithms are employed. In single phase flow, particles are added to the flow to carry out PIV or PTV. However, the foam images already provide sufficient structural information so that no particles are added in our case.

For PIV analysis, we rely on the visible network of Plateau borders through the foam sample (see Figure 2). We employ a standard PIV algorithm included in the software package PI-VLab directly on these images. For pre-processing, the wall area was masked. The interrogation window size equal 2 by 2 mm² corresponding to 64 by 64 px². The averaged velocity field was obtained from a 5 mm high (100 px) section in the middle of the spacing between the tongue and the palate.

This section then was divided into 12 equidistant radial segments. The average value of the radial component of velocity vectors in a section was determined.

For PTV measurement, the segmented images were used (see Figure 2 b,d). We utilize the center of mass of the visible bubble area to track the bubble movement. In order to generate velocity profiles averaged in space and time, the velocity of the whole bubble area was assumed to equal the center velocity. Then, the velocity in a certain region was averaged by averaging the velocities of all overlapping bubbles in radial segments, using the overlapping area as weight.

Results

Image segmentation

A typical result of the image segmentation is visible in Figure 2. In case of wet foam, the facets between bubble and front wall are very well recognized. In case of dry foam, some artefacts from back-side Plateau borders are visible. However, these can be removed by binary image treatment and do not disturb the subsequent analysis. From the size of the facettes the bubble size can be derived. However, the equivalent facet radius does not equal the equivalent bubble

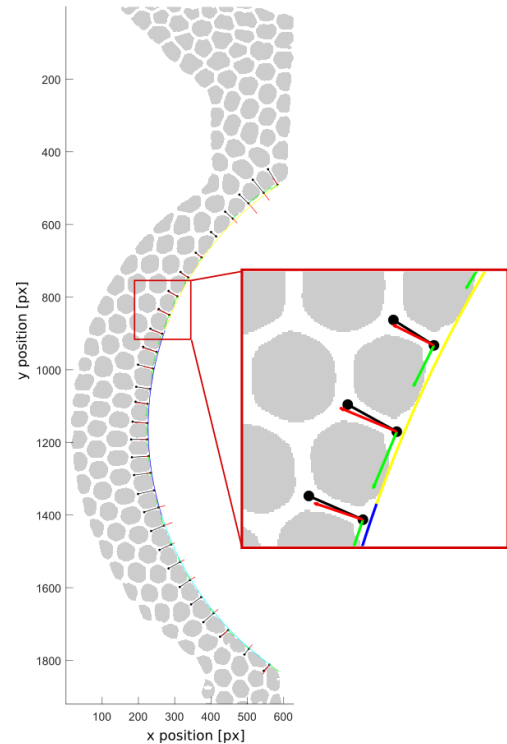


Figure 3: Sketch of identifying the tilt of the Plateau borders at the tongue surface.

radius. Wang & Neethling (2009) give a detailed description on how to transform facet size into equivalent bubble radius.

Beyond bubble size, the image segmentation also yields the amount of black area between the facets. This represents the thickness of wall-bounded Plateau borders and is directly linked to the liquid fraction of the foam (Forel et al. 2016). The segmented example images in Figure 2 hold 17 and 24 % black area, which should equal 0.5% and 1% liquid fraction, respectively. This deviates significantly from the measured values of 3.4% and 11.2%, respectively. Forel et al. used a total reflection-based frontlight illumination that makes wall-bounded Plateau borders completely dark. Our backlight illumination significantly differs from that. Thus, the image segmentation algorithm overestimates the facet size.

Foam flow velocity

Figure 4 shows example images on the result of PIV and PTV for a case with 2.35 mm bubble diameter, 20 mm/s tongue velocity and 5.8 ml/min liquid flow rate. PIV provides higher spatial resolution. However, close to the non-moving wall the velocities can be biased. PTV, on the other hand, provides only one velocity for each bubble. But, since the movement of foam is well represented by the movement of its individual bubbles, this information is sufficient to evaluate the velocity distribution.

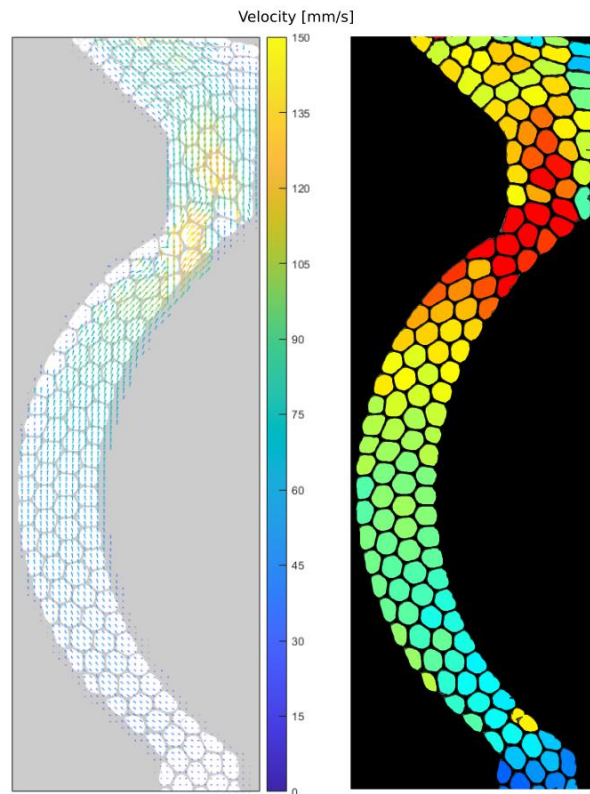


Figure 4: Velocity magnitude extracted from PIV (left) and PTV (right).

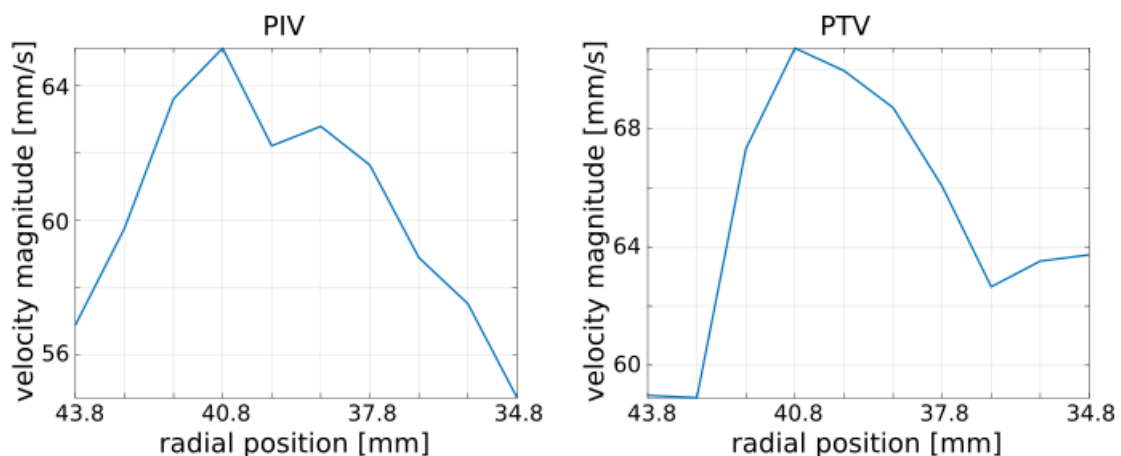


Figure 5: Radial profile of the vertical velocity of the foam for PIV (left) and PTV (right).

Subsequently, the velocity profiles along the radial position are extracted by binning and averaging the velocity information in 12 bins. Figure 5 compares the velocity profiles extracted from PIV and PTV measurements for the case in Figure 4 at the position in the middle of the tongue.

PIV results in a smooth velocity distribution while the PTV profile consists of three different velocity levels, corresponding to the lines of bubbles in Figure 4.

Wall shear stress

The wall shear depends on the friction between foam and wall. The liquid film allows for a velocity slip between foam and wall (Saughey et al. 2006). This slip can be reduced by reduced film thickness or by wall roughness. Figure 6 compares the velocity profile from PTV and the wall stress on the tongue surface between a rough and a smooth tongue for different tongue positions. In case of a rough tongue, significantly higher wall shear stress is visible which corresponds to a velocity gradient towards the tongue. Also, at the palate velocity gradient is visible for both cases. This is due to a lower liquid fraction on the palate because the draining water accumulates at the tongue due to the orientation of palate and tongue surface in the upper part of the setup (compare Figure 1).

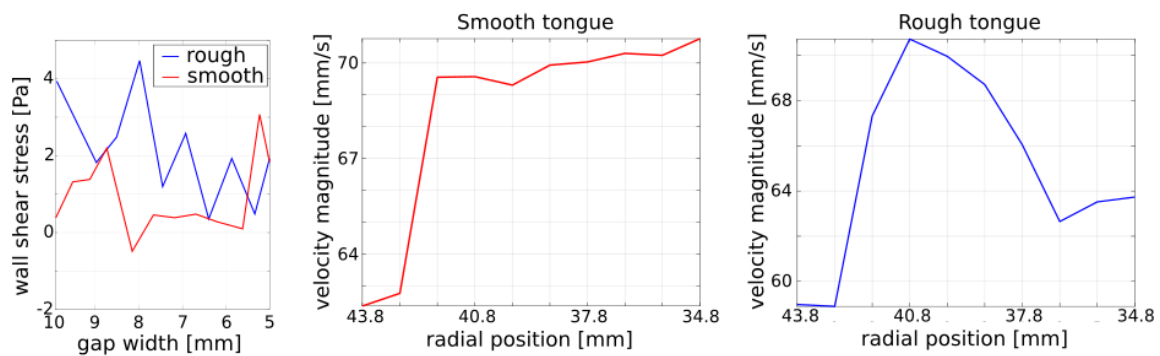


Figure 6: Wall shear stress at the tongue for different tongue positions (left) and velocity distribution in the gap between tongue and palate for smooth (center) and rough (right) tongue.

Discussion and Outlook

We have demonstrated an adapted PIV and PTV algorithm to measure the velocity distribution inside the foam flow. However, as visible in Figure 5, the velocity values between both techniques deviate by up to 10% from each other. Firstly, PIV is based on transmission images and thus, considers the full 3-dimensional flow while PTV is based on the wall surface segmentation and thus, considers flow only at the front wall. Secondly, PIV might be biased by the non-moving walls.

We have segmented the foam images successfully using a CNN approach. The resulting figures allow to estimate the local bubble size and liquid fraction and allow for bubble tracking velocimetry. Moreover, the orientation of the Plateau borders perpendicular to the wall allows for estimating the wall stress. The resulting stress is in the order of a few Pascals and thus, would be difficult to be measured directly. However, the stress values show significant oscillation, due to ongoing T1 rearrangements and limited precision of the angle determination in wet foam.

In the next step, we will systematically analyze data on different bubble size, liquid fraction, tongue roughness, tongue speed and liquid material in order to understand the behavior of food foam during the swallowing.

References

- Bourne, M. C., 2002:** "Food texture and viscosity", Food science and technology. International series
Cantat, Isabelle, et al. Foams: structure and dynamics. OUP Oxford, 2013
- Campanella, O. H.; Peleg, M., 1987:** "Lubricated squeezing flow of a Newtonian liquid between elastic and rigid plates", Rheol Acta (Rheologica Acta), Vol. 26, No. 4, pp. 396–400
- Cohen-Addad, S.; Höhler, R.; Pitois, O., 2013:** "Flow in Foams and Flowing Foams", Annu. Rev. Fluid Mech. (Annual Review of Fluid Mechanics), Vol 45, No. 1, pp. 241–267
- Dollet, B., & Graner, F. 2007.:** "Two-dimensional flow of foam around a circular obstacle: local measurements of elasticity, plasticity and flow." Journal of Fluid Mechanics, 585, 181-211
- Feitosa, K., Marze, S., Saint-Jalmes, A., & Durian, D. J. 2005.:** "Electrical conductivity of dispersions: from dry foams to dilute suspensions." Journal of Physics: Condensed Matter, 17(41), 6301
- Forel, E. et al., 2016.:** "The surface tells it all: relationship between volume and surface fraction of liquid dispersions". Soft matter, 12(38), 8025-8029
- Fox, D.; Sahin, A. W.; Schutter, D. P. de; Arendt, E. K., 2022:** "Mouthfeel of Beer: Development of Tribology Method and Correlation with Sensory Data from an Online Database", Journal of the American Society of Brewing Chemists, Vol. 80, No. 2, pp. 112-127
- Greis, M. et al., 2022:** "Physicochemical Properties and Mouthfeel in Commercial Plant-Based Yogurts", Foods (Basel, Switzerland), Vol. 11, No. 7
- Höhler, R.; Cohen-Addad, S., 2005:** "Rheology of liquid foam", J. Phys.: Condens. Matter, Vol. 17 No. 41, pp. R1041-R1069
- Knüpfer, L.; Heitkam, S., 2022:** "A machine learning approach to determine bubble sizes in foam at a transparent wall", Meas. Sci. Technol., Vol. 33, No. 6, pp. 067001
- Kokini, J. L.; Kadane, J. B.; Cussler, E. L., 1977:** "LIQUID TEXTURE PERCEIVED IN THE MOUTH", J Texture Studies, Vol. 8, No. 2, pp. 195–218
- Marchand, M.; Restagno, F.; Rio, E.; Boulogne, F., 2020:** "Roughness-Induced Friction on Liquid Foams", Physical review letters, Vol. 124, No. 11, pp. 118003
- Mathmann, K., 2010:** "Investigation of intraoral mechanical effects on sensory sensations and their contribution to mouthfeel", Technische Universität München
- Morelle, E.; Rudolph, A.; McHardy, C.; Rauh, C., 2021:** "Detection and prediction of foam evolution during the bottling of noncarbonated beverages using artificial neural networks", Food and Bioproducts Processing, Vol. 128, pp. 63–76
- Murray, B. S., 2020:** "Recent developments in food foams", Current Opinion in Colloid & Interface Science, Vol. 50, pp. 101394
- Nicosia, M. A.; Robbins, J., 2001:** "The fluid mechanics of bolus ejection from the oral cavity", Journal of Biomechanics, Vol. 34, No. 12, pp. 1537–1544
- Osei-Bonsu, K., Shokri, N., & Grassia, P. 2016:** "Fundamental investigation of foam flow in a liquid-filled Hele-Shaw cell" Journal of colloid and interface science, 462, 288-296
- Panckow, R. P.; McHardy, C.; Rudolph, A.; Muthig, M.; Kostova, J.; Wegener, M.; Rauh, C., 2021:** "Characterization of fast-growing foams in bottling processes by endoscopic imaging and convolutional neural networks", Journal of Food Engineering, Vol. 289, pp. 110151
- Rauh, C.; Singh, J.; Nagel, M.; Delgado, A., 2012:** "Objective analysis and prediction of texture perception of yoghurt by hybrid neuro-numerical methods", Int. Dairy Journal, Vol. 26, No. 1, pp. 2-14
- Ronneberger, O.; Fischer, P.; Brox, T., 2015:** "U-Net: Convolutional Networks for Biomedical Image Segmentation"
- Saughey, A., Drenckhan, W., & Weaire, D. 2006.:** "Wall slip of bubbles in foams" Physics of Fluids, 18(5), 053101
- Selway, N.; Stokes, J. R., 2014:** "Soft materials deformation, flow, and lubrication between compliant substrates: impact on flow behavior, mouthfeel, stability, and flavor", Annual review of food science and technology, Vol. 5, pp. 373–393
- Stokes, J. R.; Boehm, M. W.; Baier, S. K., 2013:** "Oral processing, texture and mouthfeel: From rheology to tribology and beyond", Current Opinion in Colloid & Interface Science, Vol. 18, No. 4, pp. 349–359
- Szczesniak, A. S., 2002:** "Texture is a sensory property", Food Quality and Preference, Vol. 13, No. 4, pp. 215–225
- Tong, M., Cole, K., & Neethling, S. J. , 2011:** "Drainage and stability of 2D foams: Foam behaviour in vertical Hele-Shaw cells". Colloids and Surfaces A: Physicochemical and Engineering Aspects, 382(1-3), 42-49.
- Wang, Y., & Neethling, S. J. 2009.:** "The relationship between the surface and internal structure of dry foam." Colloids and Surfaces A: Physicochemical and Engineering Aspects, 339(1-3), 73-81